FUNGAL BIOLOGY 118 (2014) 444–452

British Mycological Society promoting fungal science

journal homepage: www.elsevier.com/locate/funbio

Localization and speciation of arsenic in *Glomus intraradices* by synchrotron radiation spectroscopic analysis

Ma. del Carmen A. GONZÁLEZ-CHÁVEZ[a], *Bradley MILLER*[b,*], *Ignacio Eduardo MALDONADO-MENDOZA*[c], *Kirk SCHECKEL*[b], *Rogelio CARRILLO-GONZÁLEZ*[a]

[a]*Colegio de Postgraduados, Edafología, km 36.5 Carr. Mexico-Texcoco, Montecillo, Estado de México 56230, Mexico*
[b]*U.S. Environmental Protection Agency, National Risk Management Research Laboratory, Land Remediation and Pollution Control Division, Cincinnati, OH, United States*
[c]*Departamento de Biotecnología Agrícola, Instituto Politécnico Nacional, Centro Interdisciplinario de Investigación para el Desarrollo Integral Regional-IPN Unidad Sinaloa, Mexico*

ARTICLE INFO

Article history:
Received 9 September 2013
Received in revised form
28 February 2014
Accepted 6 March 2014
Available online 19 March 2014
Corresponding Editor:
Bradley W. Miller

Keywords:
Arbuscular mycorrhizal fungi
Arsenate
Arsenite
Reduction
X-ray absorption near edge spectroscopy

ABSTRACT

The protective mechanisms employed by arbuscular mycorrhizal fungi (AMF) to reduce the toxic effects of arsenic on host plants remain partially unknown. The goal of this research was identifying the *in situ* localization and speciation of arsenic (As) in the AM fungus *Rhizophagus intraradices* [formerly named *Glomus intraradices*] exposed to arsenate [As(V)]. By using a two-compartment *in vitro* fungal cultures of *R. intraradices*-transformed carrot roots, microspectroscopic X-ray fluorescence (μ-XRF), and microspectroscopic X-ray absorption near edge structure (μ-XANES), we observed that As(V) is absorbed after 1 h in the hyphae of AMF. Three hours after exposure a decrease in the concentration of As was noticed and after 24 and 72 h no detectable As concentrations were perceived suggesting that As taken up was pumped out from the hyphae. No As was detected within the roots or hyphae in the root compartment zone three or 45 h after exposure. This suggests a dual protective mechanism to the plant by rapidly excluding As from the fungus and preventing As translocation to the plant root. μ-XANES data showed that gradual As(V) reduction occurred in the AM hyphae between 1 and 3 h after arsenic exposure and was completed after 6 h. Principal component analysis (PCA) and linear combination fitting (LCF) of μ-XANES data showed that the dominant species after reduction of As(V) by *R. intraradices* extra-radical hyphal was As(III) complexed with a reduced iron(II) carbonate compound. The second most abundant As species present was As(V)–iron hydroxides. The remaining As(III) compounds identified by the LCF analyses suggested these molecules were made of reduced As and S. These results increase our knowledge on the mechanism of As transport in AMF and validate our hypotheses that *R. intraradices* directly participates in arsenic detoxification. These fungal mechanisms may help AMF colonized plants to increase their tolerance to As at contaminated sites.

* *Corresponding author*. Present address: U.S. Environmental Protection Agency, National Enforcement Investigations Center, PO Box 25227, Denver, CO 80225, United States. Tel.: +1 303 462 9150; fax: +1 303 462 9028.
E-mail addresses: carmeng@colpos.mx (M. C. A. González-Chávez), Miller.BradleyW@epa.gov (B. Miller), imaldona@ipn.mx (I. E. Maldonado-Mendoza), Scheckel.Kirk@epa.gov (K. Scheckel), crogelio@colpos.mx (R. Carrillo-González).
1878-6146/$ – see front matter Published by Elsevier Ltd on behalf of The British Mycological Society.
http://dx.doi.org/10.1016/j.funbio.2014.03.002

Introduction

Arbuscular mycorrhizal fungi (AMF) are the dominant beneficial symbionts colonizing roots of more than 90 % of the world's plant genera (Smith & Read 2008). In metal(loid) polluted soils, many plant species adapted to grow on these sites are colonized by these fungi possibly playing a central role in ameliorating toxicity of these pollutants (Zarei *et al.* 2008; González-Chávez *et al.* 2009; Ortega-Larrocea *et al.* 2010). Since AMF have a predominant role in acquiring phosphate for mycorrhizal associations and arsenate is a chemical analogue of phosphate, it might appear paradoxical that AMF potentially enhance arsenate uptake while also increasing arsenate tolerance for the plant host (González-Chávez *et al.* 2002, 2011; Smith *et al.* 2010). Recent research has focused on the effects of As accumulation and growth of mycorrhizal plants compared to non-mycorrhizal plants, as well as the effects of As on fungal colonization (Ahmed *et al.* 2006; Chen *et al.* 2007; Xia *et al.* 2007; Dong *et al.* 2008). The protective mechanisms employed by AMF to reduce the toxic effects of As on host plants remain unknown. Meharg (2003) suggested that mycorrhizal fungi employ the same mechanisms found in other microorganisms to reduce the toxic effects of As by relying on As exclusion. Meharg (2003) hypothesized that the fungus achieves As resistance by reducing arsenate (As(V)) to arsenite (As(III)) followed by actively pumping As(III) out of the fungal cells. In a study on arsenate resistance of *Holcus lanatus* conferred by AMF, González-Chávez *et al.* (2002) found that all AMF strains tested conferred additional As tolerance. They suggested that arsenate influx was reduced in *H. lanatus* plant roots by the suppression of high-affinity arsenate/phosphate transporters thereby decreasing arsenate uptake. Ultra *et al.* (2007) hypothesized that AMF may be involved in the transformation of inorganic As to less toxic organic forms which consequently led to decreased As uptake by sunflower plants. A limitation of these studies was no way to delineate the plant host or AMF As detoxification mechanisms.

More recently, our research group identified a gene with high similarity to a putative As efflux pump (GiArsA) expressed in arbuscules and the extra-radical hyphae of *Rhizophagus intraradices* [formerly named *Glomus intraradices*] (González-Chávez *et al.* 2011). Based upon González-Chávez *et al.* (2011) we proposed the following As detoxification mechanism in fungi. First, As(V) absorbed by the fungal hyphae symbiont *via* a high-affinity phosphate transporter (GiPT) is transformed by a still unknown putative As(V) reductase to produce As(III). Next, the As(III) is translocated to the extra-radical hypha and effluxed outside the plant's rhizosphere by a membrane-bound As(III) pump designated GiArsA/B. However, without evidence, our hypothesis was the reduction, translocation, and elimination of As(III) as a detoxification effect on the plant host thereby increasing the fitness of both symbionts and enhancing plant As tolerance.

The goal of this research was to acquire more information on the possible mechanisms AMF evolved in arsenic tolerance through the *in situ* localization and speciation of As in the AM fungus *R. intraradices* and mycorrhizal roots exposed to As(V). Rates of As uptake were reported in (González-Chávez *et al.* 2011). Under the proposed molecular model for *R. intraradices* about As detoxification (González-Chávez *et al.* 2011), the present research gives additional *in situ* data on As localization and speciation supporting the molecular evidence and validating our proposed model for arsenate transport in arbuscular mycorrhiza: *R. intraradices* is able to reduce As(V) and pump it out from the extra-radical mycelium.

Material and methods

Transformed carrot roots-Rhizophagus intraradices arbuscular mycorrhizal cultures

Plant material, fungal species, and axenic cultures used in this study were the same as reported by González-Chávez *et al.* (2011). Briefly, two-compartment Petri dishes containing transformed carrot root-*R. intraradices* arbuscular mycorrhizas were established (Fig S1A, Supplementary data). The plant compartment containing solid M medium (St-Arnaud *et al.* 1996) was inoculated with roots and 2 weeks later, they were inoculated with *R. intraradices* spores. At 3 weeks after inoculation, M solid medium without sucrose was added to the second compartment. The plates were incubated in the dark at 25 °C. After 4 weeks, extra-radical hyphae were developed around the roots in the first compartment (root-hyphae compartment; RHC) and grew into the solid media in the second hyphal compartment (HC). At this stage, colonization of the roots was estimated by the modified grid-intersect method (McGonigle *et al.* 1990), and the average colonized root length was 56 %, with an average deviation from the mean of 10 %. At this point (10 weeks of culture), phosphate was depleted from the solid media (Maldonado-Mendoza *et al.* 2001). Plates of this age and phosphate condition were used in all experiments. This unique system allowed us to conduct the current *in situ* study.

Time-course kinetics for arsenate exposure

A dose of 350 μM arsenate (NaH_2AsO_4) was directly added *via* a pipette to plates containing abundant extra-radical hyphae (≈10 mg) in the HC. The time-course reactions were established at 0, 1, 3, 6, 24, and 72 h and the resultant treatments were: (1) the extra-radical hyphae from HC; which were directly treated with arsenate; (2) the extra-radical hyphae and mycorrhizal roots from RHC; which might receive arsenate indirectly by the hyphae from the HC. Reactions were stopped at the different times by separating the extra-radical mycelium or colonized roots from the solid medium. This was done carefully and avoiding disturbance by cutting with a scalpel the solid medium from both compartments. Extra-radical hyphae or mycorrhizal roots were separated by hydrolyzing the medium with a 10 mM citric acid solution for approximately 1 min followed by filtration through a 30 μm nylon mesh, rinsed three times with sterile and deionized water, and carefully dried with paper towel. Vital staining of fungal hyphae was carried out in all the experiments by nitro blue tetrazolium (NBT)-succinate test (Schaffer & Peterson 1993). Experiments were performed twice using three biological replicates each time with similar results. Data sets from

a single experiment are shown. Fungal tissue at 24 and 72 h was inspected under the light microscope at 100 and 400× to check for bacterial contamination. No obvious signs of other microorganism contamination were observed. In parallel experiments bacterial contamination has been discarded by plating in Luria Bertani medium (LB) and potato dextrose agar medium (PDA) rich media the M medium surrounding the external hyphae.

In situ *micro-XAFS and micro-XRF analyses*

One can employ an array of techniques to address speciation; however, true *in situ* analysis is limited to a few options such as advanced synchrotron radiation methods to elucidate metal speciation and distribution (Scheckel 2006). High-energy synchrotron X-rays were used to attain *in situ* atomic level information on the distribution and speciation of arsenic in the extra-radical hyphae of *Rhizophagus intraradices* and mycorrhizal colonized roots. Microspectroscopic X-ray fluorescence (μ-XRF) and microspectroscopic X-ray absorption near edge structure (μ-XANES) spectra were collected at Sector 20-ID (PNC/XOR) at the Advanced Photon Source, Argonne National Laboratory operating at 7 GeV in top-up mode. Sector 20-ID uses a liquid nitrogen cooled Si (1 1 1) double crystal monochromator that was calibrated using American Chemical Society (ACS) grade sodium arsenate (11 874 eV).

The hyphal mass, from HC compartment obtained from the time-course experiments, was first inspected under a dissecting scope (Fig S1B and C, Supplementary data), and then mounted within two pieces of Kapton tape. The taped samples were initially mounted within a Linkam® cryostat stage to prevent beam-induced artifacts; however, ice formation on the stage window prevented the use of the cryostat. Instead, the taped samples were mounted on a sample holder and placed directly in the beam for analyses.

Large μ-XRF maps (1000 μm^2) of the fungal biomass were collected at 12 200 eV with 10 μm steps at 0.5 s integration for elemental distribution including As and Fe. After As hot spots were located, small μ-XRF maps were collected at 50 μm^2 with 5 μm steps and 0.3 s integration time. Once As hot spots were determined on the small μ-XRF maps, μ-XANES spectra were collected at 0.5 eV steps around the absorption edge −10 through 30 eV (full scans −150 through 500 eV) with an ACS grade sodium arsenate (11 874 eV) reference for calibration. The μ-XRF maps and μ-XANES spectra were collected in fluorescence mode using a Vortex-ME4 four-element silicon drift detector. μ-XANES spectra with absorption edge steps <0.01 units were considered to be below the detection limit in our experiments and no further analyses were performed. μ-XRF mapping and μ-XANES analyses were collected in the HC of samples 1, 3, 6, 24, and 72 h after As(V) addition. μ-XRF mapping and μ-XANES analyses from tissue masses containing roots and hyphae from RHC 3 and 45 h after exposure to As(V) in the hyphal zone (HC) were also collected.

Preliminary results demonstrated that beam-induced reduction of As(V) within the fungal samples had occurred during μ-XANES analyses (Fig S2, Supplementary data). Therefore one or two scans were collected at multiple spots for each sample, the energy was calibrated against sodium arsenate standard for each sample then merged (if no reduction was detected), and normalized using Athena software (Ravel & Newville 2005). Principal components analyses (PCAs) were performed in Sixpack (Webb 2005) on the normalized scans and target factor analyses of each arsenic standards were performed to determine the most appropriate standards to be used for linear combination fitting (LCF) analyses. Eighteen As standards were analyzed including a mix of minerals and organic As compounds were used for target factor analysis. Supplemental Table S1 lists the standards, peak positions, and SPOIL values derived from our PCAs. Six As standards with SPOIL values less than 3.0 were used in the LCF analyses including arsenite sorbed to siderite, arsenite sulfide, arsenopyrite, dimethylarsinic acid (DMA), sodium arsenate, and arsenate sorbed to ferrihydrite (Table S1, Supplementary data). The LCF models were fit using the normalized and derivative spectra at −10 to 25 eV relative to the absorption edge, standards were not constrained to using a single E0 shift, and weighting factors were constrained to values between 0 and 1, and 'Fit All Combinations' with at most 3 standards. The results of the LCF analyses generated models with the best fit indicated by the lowest *R*-factor and reduced chi square values. The LCF models predict the As speciation at each spot within the hyphal mass as percentages of the reference arsenic standards. Predicted As phases within the hyphal mass are dependent upon the *a priori* choice of As standards. There are many different As biochemical compounds and previous research has demonstrated the difficulty of resolving these compounds with XANES analysis (Smith *et al.* 2005). Therefore we will refer to the results of the LCF fitting as As(III) iron carbonate (arsenite sorbed to siderite), As(III) sulfide (arsenite sulfide), As(III) iron sulfide (arsenopyrite), DMA, sodium arsenate (NaAs(V)), and As(V) sorbed iron hydroxide (arsenate sorbed to ferrihydrite) (Fig S3, Supplementary data).

Results

μ-XRF mapping

Elemental mapping of *Rhizophagus intraradices* demonstrated an uptake of As soon after the extra-radical hyphae were spiked with As(V) in the HC, but the concentration of As declined over 24 h. There was no As fluorescence from the extra-radical hyphae in the control plates but Fe fluorescence appears diffuse throughout the extra-radical mycelium (Fig 1). One hour after As(V) was added to the HC, As and Fe fluorescence appear diffuse throughout more than 80 % of the mapped area. The relationship between As and Fe fluorescence decreased 3 h after As(V) addition, with few areas of co-occurrence between As and Fe at 6 and 24 h after spiking. After 24 h the majority of As has been effluxed out from the extra-radical mycelium and washed away. The Fe appears to have remained within the extra-radical mycelium and accumulated on globular surface of spore walls appearing greenish yellow (in the web version) in Fig 1 plate 24 h. Through 24 h of exposure, As never appeared to be stored in the extra-radical mycelium or spores (Fig 1).

Many unsuccessful attempts were made to detect As in the RHC at 3 and 45 h after As(V) additions. Root tips were selected nearest the HC with the intention of maximizing the

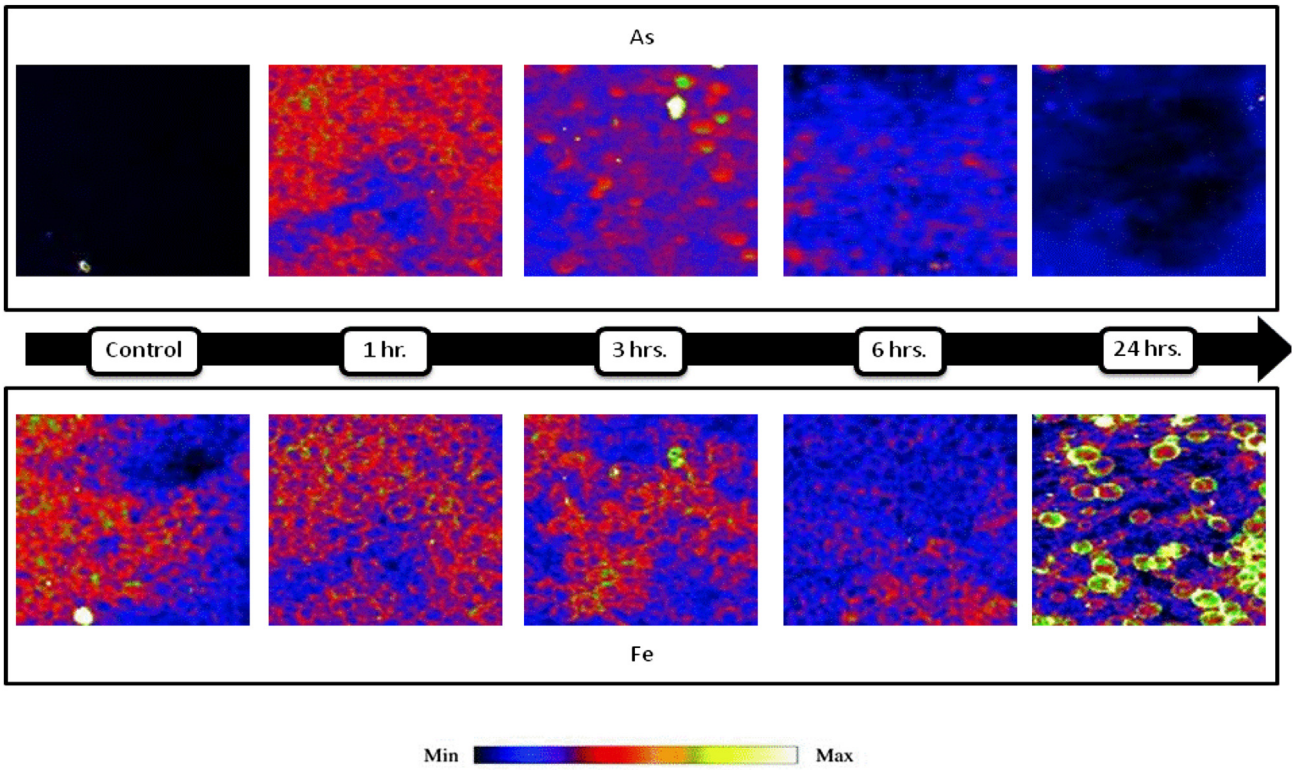

Fig 1 – Elemental mapping of five different *Glomus intraradices* extra-radical hyphae masses exposed to As(V) over 24 h. Each image is 1000 × 1000 μm (10 μm steps with 0.5 s integration). The colour is in arbitrary units: black and white corresponding to the lowest and highest relative concentrations. (For interpretation of the references to colour in this figure legend, the reader is referred to the web version of this article.).

likelihood of detecting transported As. Additionally, μ-XRF mapping was performed on sparsely spaced individual hyphal strands; however, the As concentrations were below detection. White hot spots, like the one shown in the control images (Fig 1) and 3 h after As(V) addition, have abnormally high concentrations of all elements mapped and are likely from exaggerated X-ray absorption of denser entrained agarose gel not washed away (Fig S4, Supplementary data).

μ-XANES analyses

The As(V) spiking solution was analyzed and determined to only contain As(V) (Fig 2). Arsenic was reduced to As(III) within 1 h of As(V) addition to the HC. The μ-XANES spectra suggest and PCAs confirmed that as many as two As species were detected in the spectra collected at the eight spots analyzed (Fig 2). Following μ-XRF mapping of the *Rhizophagus intraradices* extra-radical mycelium after 1 h, μ-XANES analyses and LCF predictions suggest that >50 % of the As present was As(III). Similarly 3, 6, or 24 h after As(V) addition, the dominant As species remained as As(III) followed by As(V) (Table 1).

The LCF results suggest that the dominant arsenic species present in the extra-radical mycelium most closely matched the standard As(III) bound to an iron(II) carbonate (Table 1). Following As(III), the dominant species present at each spot was predicted to be As(V) bound as an iron(III)-hydroxide like compounds. Three times (1, 6, and 24 h) throughout the experiment, other reduced As(III) phases were predicted to be present, notably As(III) bound to sulphur compounds (Table 1).

Discussion

μ-XRF

Arsenic accumulation and transformation are dynamic and complicated process, which cannot be simply explained by the total arsenic concentration detected at a specific time (Li *et al.* 2012). Likewise, different As species in the environment may affect the exposure response of *Rhizophagus intraradices* and the host plants. Our results were taken during a time-course experiment in order to gain a better understanding of the As transport mechanisms occurring in an AMF. Arsenate appears uniformly throughout the extra-radical mycelium 1 h after exposure to As(V) spiking solution (Fig 1). Scans collected 3 h after exposure showed a decrease in the concentration of As suggesting that As that had been absorbed was effluxed from the hyphae and washed away during the dissolution of the agar. The mapped μ-XRF images at both 5 and10 μm step sizes showed a very diffuse distribution of As. Therefore it suggests that As was not stored within extra-radical mycelium or spores.

While As uptake was fast, it was also rapidly pumped out from the extra-radical mycelium. The marked decrease in As beginning 3 h after exposure and the undetectable As

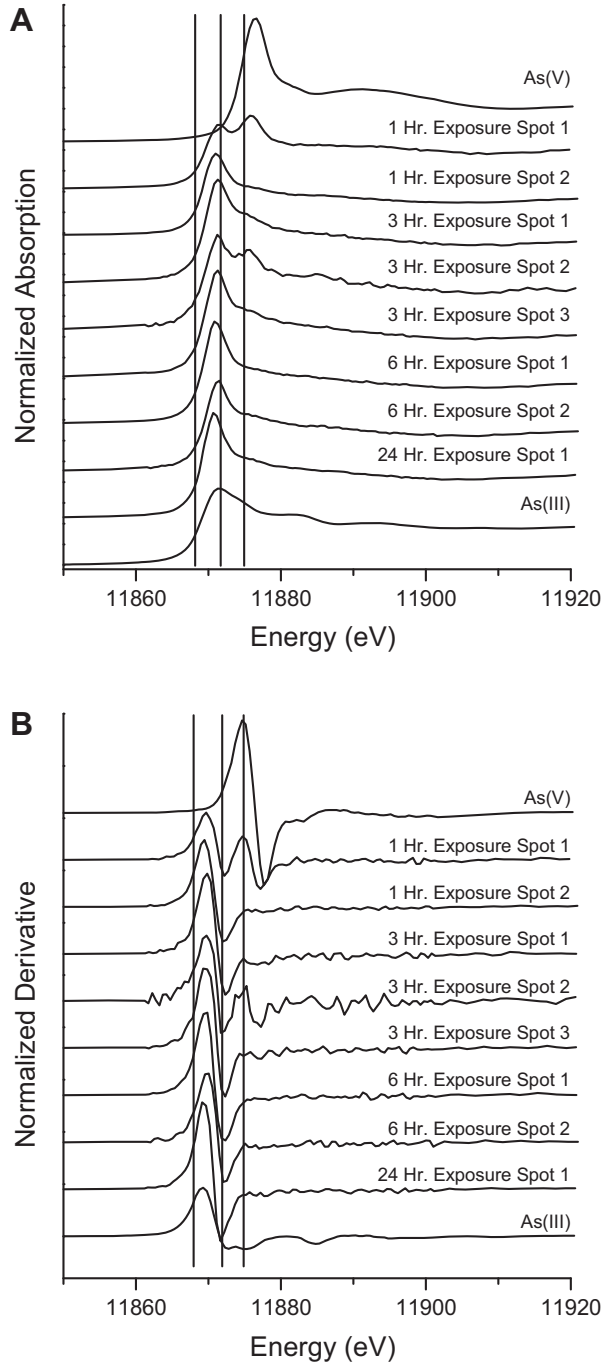

Fig 2 – Normalized (A) and derivativized (B) μ-XANES data of *Glomus intraradices in vivo* reduction of arsenate over time. The vertical lines are at 11 868, 11 870, and 11 875 eV.

concentrations at 24 and 72 h demonstrates that *R. intraradices* is not retaining detectable concentrations of As within fungal tissues. Further, detectable concentrations were not noticed for As absorbed within cell walls of the hyphae or spores after 24 h of exposure unlike iron (Fig 1).

Previous research has documented the potential for As adsorption to fungal walls and spores of filamentous fungi (Gadd 2004; Srivastava *et al.* 2011). However, in this study it is highly unlikely that As would remain adsorbed to fungal walls. The high ionic strength of the citrate washing solution (10 mM) used to obtain the extra-radical hyphae masses would through mass action remove As anions from these surfaces and complex any bridging cations coupling As to fungal walls.

When As was supplemented to the HC, no As was detected within the roots or the extra-radical mycelium in the RHC. We attempted to identify As within the RHC of the cultures 3 and 45 h after exposure to As(V) without any success. The rapid exclusions of the absorbed As would limit toxicity to both symbionts. These results suggest either the fungus prevented As translocation to the plant root, or if there was As transportation to the root, it was undetectable in our experiment. Both scenarios result in the fungus providing dual protective mechanisms to the plant. First, As(V) in many plants can be absorbed in the same transport channels used for P uptake (Ullrich-Eberius *et al.* 1989; Meharg & Hartley-Whitaker 2002; Shin *et al.* 2004). Rapid absorption of As(V) and reduction to As(III) by *R. intraradices* extra-radical mycelium or arbuscules within the root may reduce As(V) availability and hence As(V) uptake directly by plant P transporters. This mechanism is similar to the As exclusion mechanism suggested in ericoid mycorrhizal fungi by Sharples *et al.* (2000). Second, As taken up by *R. intraradices* appears to be rapidly excluded out of the fungus and not transported back to the root with water and beneficial nutrients. Rapid uptake by the fungal symbiont and reduction of As(V) decreases the likelihood of exposure to the host plant, which would decrease the health impacts to both symbionts. This is in accordance to Smith *et al.* (2010), indicating that As is not transferred to the root cells themselves or translocated to the shoots. Low arsenic translocation may also be a mechanism restricting root As uptake and conferring enhanced host plant tolerance as suggested by Xu *et al.* (2008) and Chen *et al.* (2007). Several authors have reported lower As concentrations in AM roots than non-mycorrhizal roots and consequently in shoots (González-Chávez *et al.* 2002; Leung *et al.* 2006; Chen *et al.* 2007) which would alleviate As toxicity in mycorrhizal roots.

μ-XANES

Reduction of arsenate followed by efflux of As(III) is an important mechanism of arsenic tolerance employed by microorganisms (Salt & Norton 2008). In relation to this, several authors have suggested that AMF might increase the efflux of As(III) from mycorrhizal roots (González-Chávez *et al.* 2002, 2011; Chen *et al.* 2007; Smith *et al.* 2010); however, no direct evidence of arsenic reduction by AMF has been reported previously. Our results demonstrate conclusively that *Rhizophagus intraradices* is responsible for the reduction of As(V) in the extra-radical hypha. Previous research has demonstrated that *R. intraradices* expresses a gene with high similarity to a putative As efflux pump (*GiArsA*) in arbuscules and the extra-radical hyphae (González-Chávez *et al.* 2011). Previous research (Sharples *et al.* 2000) has also shown As reduction within an hour of exposure by an ericoid mycorrhizal symbiont: *Hymenoscyphus ericae*, isolate cultured from As contaminated soil. Rapid uptake and reduction could be beneficial to the host plant if As(III) is not readily absorbed by the plant. However, As(III) is more mobile than As(V) in acidic soils and

Table 1 – Results of LCF models and prediction of minerals present (%).

Arsenic exposure to HC		LCF results					R-factor	Reduced chi sq.
Time elapsed	Location of scan	As(III)–iron carbonate	As(III)–iron sulphate	As(III)–sulfide	As(V)–iron hydroxide	Na As(V)		
0 h	Solution	–	–	–	–	100 %	–	–
1 h	Spot 1	54 %	–	–	46 %	–	0.0027	0.0034
1 h	Spot 2	80 %	–	20 %	–	–	0.0032	0.0030
3 h	Spot 1	89 %	–	–	11 %	–	0.0014	0.0024
3 h	Spot 2	59 %	–	–	41 %	–	0.0033	0.0084
3 h	Spot 3	92 %	–	–	8 %	–	0.0010	0.0017
6 h	Spot 1	92 %	8 %	–	–	–	0.0012	0.0019
6 h	Spot 2	88 %	–	–	12 %	–	0.0027	0.0044
24 h	Spot 1	77 %	–	23 %	–	–	0.0017	0.0027
72 h		Below detection limits						

controlled in part by Fe-minerals (Herbel & Fendorf 2006; Mitsunobu *et al.* 2008). Therefore, depending upon *in situ* conditions reduction to As(III) may increase the leaching of As out of the rhizosphere, thus increasing the potential health of both symbionts.

Our results suggest the dominant species present after reduction of As(V) by *R. intraradices* extra-radical hyphae was As(III) complexed with a reduced iron(II) carbonate compound (Table S1, Supplementary data). Previous research has demonstrated the difficulty of resolving different biological As compounds with μ-XANES analysis (Smith *et al.* 2005); furthermore, the determination of As speciation is limited to the reference materials utilized and we did not have a large variety of reduced As organic standards in our study. However, fungi are capable of precipitating a variety of oxide and carbonate minerals in soil when grown in axenic conditions (Magyarosy *et al.* 2002; Burford *et al.* 2003; Miyata *et al.* 2004; Fomina *et al.* 2007; Gadd 2007). Further analyses are needed to confirm the exact forms of As(III) complexed with a reduced iron(II) carbonate.

After As(III)–iron carbonate adsorption, the most abundant As species present in fungal tissues was As(V)–iron hydroxides. The presence of As(V) bound to iron compounds was expected since these cultures were grown in an oxidizing environment in the presence of Fe. We cannot say with absolute confidence that this pool of As(V) bound to iron was within or outside the extra-radical mycelium. However, citrate is capable of chelating Fe and dissolving of amorphous iron oxides (Cornell & Schwertmann 2003) resulting in the concurrent release of As. It therefore seems most probable that the As(V)–iron hydroxide is within the fungus as the μ-XRF maps (Fig 1) clearly show consistent Fe signals before and after citrate exposure.

Wright & Upadhyaya (1996) reported that the extra-radical mycelium produces a glycoprotein (glomalin) which accumulates abundantly outside of the extra-radical mycelium during active fungal growth. Glomalin is rich in iron, hence this fungal product may be related with As in a manner analogous to iron plaque observed on root surfaces. This has been reported in many wetland plants and correlated to arsenic tolerance (Meng *et al.* 2002; Chen *et al.* 2005). Iron oxides have high affinity for this element, being greater for As(V) than for As(III) (Meng *et al.* 2002). Li *et al.* (2012) reported that rice genotype TD71 forms more iron plaque on its root surface whilst possessing greater arsenic tolerance than the Xiushui11 rice genotype. However, further work is needed to learn if glomalin is involved in metal tolerance as iron plaque in roots.

The remaining As(III) compounds identified by the LCF analyses suggested these compounds were made of reduced As and S (Table 1). Within the fungal hyphae there are a variety of intracellular detoxification mechanisms including metallothioneins, phytochelatins, methylation, and sequestration within vacuoles filled with other elements (Burford *et al.* 2003). Further research, such as performing Fe μ-XANES analyses, would be useful to confirm the production of As(III)-siderite and other predicted As species associated with Fe. However, a common detoxification of As by organisms is achieved by methylation of As(V) to form DMA or monomethylarsinic acid (MMA) (Smedley & Kinniburgh 2002). Our analyses demonstrated that neither of these organic As species were detected in the extra-radical mycelium because the As(V) was reduced to As(III). This is in contrast with results of Ultra *et al.* (2007), who reported that DMA was detected only in AM treatments and that mycorrhizal roots colonized by *Glomus aggregatum* were primarily involved, in its formation. However, single activity for the extra-radical mycelium from the root plant was not tested and comparisons are difficult.

Su *et al.* (2011) followed arsenic biotransformation by arsenic-resistant filamentous fungi, such as: *Trichoderma asperellum* SM-12F1, *Penicillium janthinellum* SM-12F4, and *Fusarium oxysporum* CZ-8F1. These authors reported a rapid biotransformation of As(V) to As(III) in the fungal media 2 or 3 d after exposure. *F. oxysporum* CZ-8F1 reduced the As(V) the quickest (2 d). These authors suggested that these fungi could be applied to the future remediation of arsenic-contaminated soils. Our results show that arsenic reduction in the extra-radical hyphae of *R. intraradices* occurs even faster (from 1 to 6 h) than in these other fungi, and it is possible that this can occur even more readily than in 1 h. Future work should involve a shorter time-course experiment between 0 and 1 h.

Finally, this research shows clear evidence of As(V) reduction and increases the information related to the mechanisms of AMF to enhance As tolerance in mycorrhizal plants (Fig 3) as follows: (1) The scheme shows that As(V) uptake in AMF hyphae is mediated *via* a high-affinity phosphate transporter (GiPT) located in hyphae and arbuscules inside

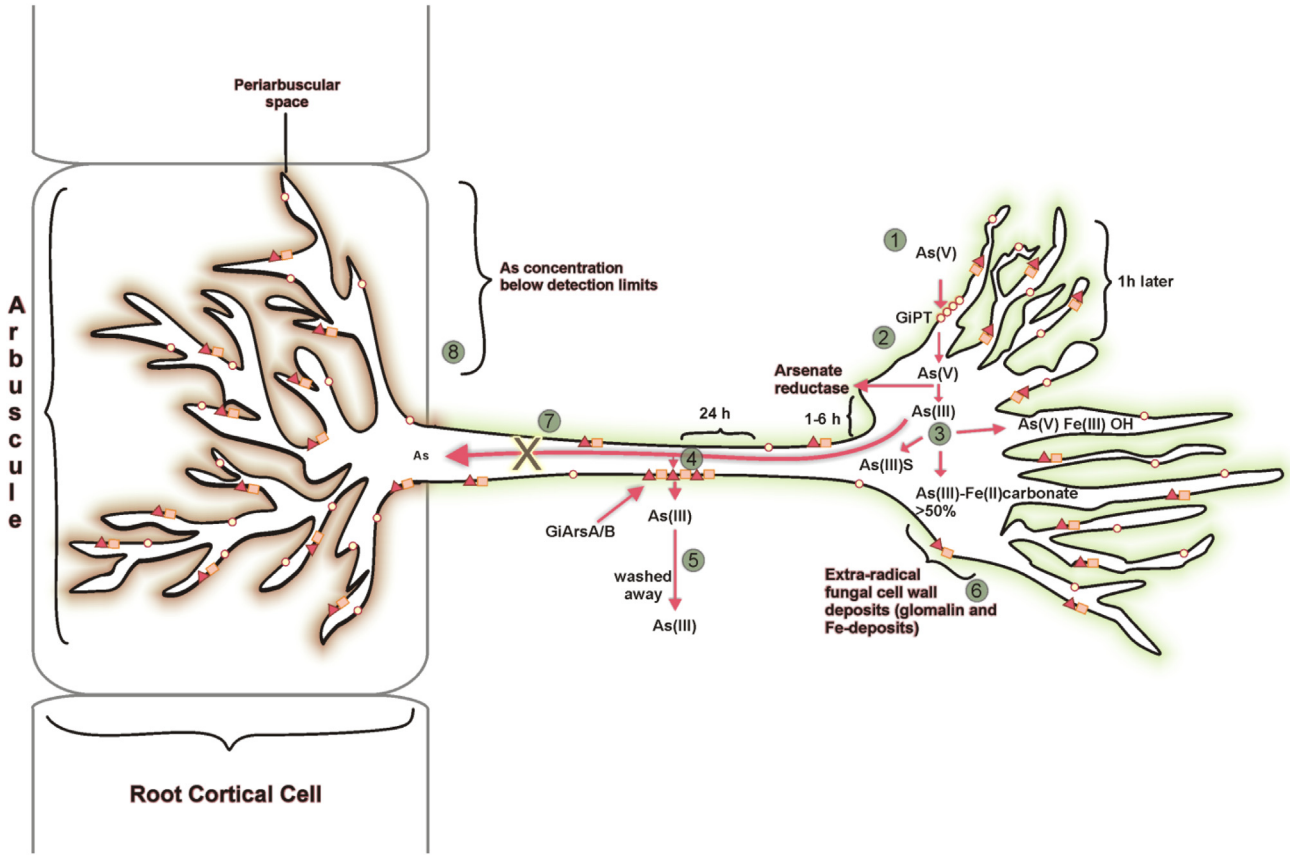

Fig 3 – Current working model for As transport and speciation mechanisms in arbuscular mycorrhiza. (1) As(V) uptake in AMF hyphae mediated *via* a high-affinity phosphate transporter (GiPT) located in hyphae and arbuscules inside the root cortical cells. (2) Reduction to As(III) possibly by an arsenate reductase. (3) As in different compounds. (4) As lower to undetectable levels. (5) As(III) excluded out of the hypha and probably leaching away from the rhizosphere. (6) Fe and compounds containing As such as glomalin are deposited in the hyphae. (7) Avoidance/reduction As translocation to the arbuscules in the root cortical cells and (8) low As accumulation in the plant root tissues, less toxicity to the photobiont, and high As plant tolerance in mycorrhizal plants.

the root cortical cells (González-Chávez *et al.* 2011). (2) Once As(V) enters the fungal hypha it is reduced to As(III) possibly *via* a still undescribed arsenate reductase. This process takes between 0 and 1 h after As(V) exposure. (3) As is found from 1 to 6 h as different compounds being the most dominant species an As(III)–Fe(II) carbonate form followed by less abundant forms such as As(V)–Fe(III) hydroxide and As(III)–sulphur compounds. (4) After 24 h exposure, As was undetectable. This might be mediated by an arsenite efflux pump which expression is induced 3 h after As exposure found in hyphae and arbuscules. (5) As(III) excluded out of the hypha is more mobile than As(V) and favour leaching of As away from the rhizosphere. (6) Fe and compounds containing As such as glomalin are deposited in the hyphae. (7) This exclusion mechanism avoids/reduces As translocation to the arbuscules in the root cortical cells and (8) ultimately prevents accumulation in the plant root tissues decreasing toxicity to the photobiont, and increasing the plant tolerance to As when associated to AMF.

These results are the basis for the potential role of AMF in bioremediation strategies combining them with plant species which could be used as plant coverage of polluted soil, or mine residues, but are not normally considered for its use due to As toxicity.

Conclusions

Our results have revealed more of the underlying mechanisms that explain better the protective role of AMF for their host plants under arsenic contamination. This work, in conjunction with the results from González-Chávez *et al.* (2011) provides evidence that a rapid reduction to As(III) and subsequent efflux of arsenic occurs directly from the extraradical hyphae of *Rhizophagus intraradices*. These results also help to explain how AM fungi may contribute to lower internal concentrations and availability for transfer of arsenic to the host roots. The innovative research tools used in this research, μ-XRF mapping and μ-XANES analyses, helped to decipher AMF As-speciation mechanisms and its involvement in As detoxification mechanisms where iron is playing a relevant role.

Acknowledgements

We thank M.Sc. Juan Carlos Martínez-Álvarez for his technical assistance in the preparation of mycorrhizal monoxenic fungal cultures. Critical review from Dr. Richard Loeppert is recognized. This project was partially supported by the Collaborative Research Grant Program Texas A&M-CONACyT (2009-021). This work was performed at the XSD/PNC Sector 20 beamline of the Advanced Photon Source (APS) of Argonne National Laboratory (Argonne, IL) through the contract no. DE_AC02-06CH11357.

Although EPA contributed to this article, the research presented was not performed by or funded by EPA and was not subject to EPA's quality system requirements. Consequently, the views, interpretations, and conclusions expressed in this article are solely those of the authors and do not necessarily reflect or represent EPA's views or policies.

Appendix A. Supplementary data

Supplementary data related to this article can be found at http://dx.doi.org/10.1016/j.funbio.2014.03.002.

REFERENCES

Ahmed FRS, Killman K, Alexander I, 2006. Influences of arbuscular mycorrhizal fungus *Glomus mosseae* on growth and nutrition of lentil irrigated with arsenic contaminated water. *Plant and Soil* **258**: 33–41.

Burford EP, Kierans M, Gadd GM, 2003. Geomycology: fungi in mineral substrata. *Mycologist* **17**: 98–107.

Cornell RM, Schwertmann U, 2003. *The Iron Oxides: structure, properties, reactions, occurrences, and uses* 2nd, completely rev. and extended edn.. Wiley-VCH, Weinheim.

Chen Z, Zhu YG, Liu WJ, Meharg AA, 2005. Direct evidence showing the effect of root surface iron plaque on arsenite and arsenate uptake into rice (*Oryza sativa*) roots. *New Phytologist* **165**: 91–97.

Chen B, Xiao X, Zhu Y-G, Smith FA, Xie ZM, Smith SE, 2007. The arbuscular mycorrhizal fungus *Glomus mosseae* gives contradictory effects on phosphorus and arsenic acquisition by *Medicago sativa* Linn. *Science of the Total Environment* **379**: 226–234.

Dong Y, Zhu Y-G, Smith FA, Wang Y, Chen B, 2008. Arbuscular mycorrhiza enhanced arsenic resistance of both white clover (*Trifolium repens* Linn.) and ryegrass (*Lolium perenne* Linn.) plants in an arsenic-contaminated soil. *Environmental Pollution* **155**: 174–181.

Fomina M, Charnock JM, Hillier S, Alvarez R, Gadd GM, 2007. Fungal transformations of uranium oxides. *Environmental Microbiology* **9**: 1696–1710.

Gadd GM, 2004. Microbial influence on metal mobility and application for bioremediation. *Geoderma* **122**: 109–119.

Gadd GM, 2007. Geomycology: biogeochemical transformations of rocks, minerals, metals and radionuclides by fungi, bioweathering and bioremediation. *Mycological Research* **111**: 3–49.

González-Chávez MC, Harris PJ, Dodd J, Meharg AA, 2002. Arbuscular mycorrhizal fungi confer enhanced arsenate resistance on. *Holcus lanatus*. *New Phytologist* **155**: 163–171.

González-Chávez MC, Carrillo-Gonzalez R, Gutierrez-Castorena MC, 2009. Natural attenuation in a slag heap contaminated with cadmium: the role of plants and arbuscular mycorrhizal fungi. *Journal of Hazardous Materials* **161**: 1288–1298.

González-Chávez MdCA, Ortega-Larrocea MdP, Carrillo-González R, López-Meyer M, Xoconostle-Cázares B, Gomez SK, Harrison MJ, Figueroa-López AM, Maldonado-Mendoza IE, 2011. Arsenate induces the expression of fungal genes involved in As transport in arbuscular mycorrhiza. *Fungal Biology* **115**: 1197–1209.

Herbel M, Fendorf S, 2006. Biogeochemical processes controlling the speciation and transport of arsenic within iron coated sands. *Chemical Geology* **228**: 16–32.

Leung HM, Ye ZH, Wong MH, 2006. Interactions of mycorrhizal fungi with *Pteris vittata* (As hyperaccumulator) in As-contaminated soils. *Environmental Pollution* **139**: 1–8.

Li H, Man YB, Ye ZH, Wu C, Wu SC, Wong MH, 2012. Do arbuscular mycorrhizal fungi affect arsenic accumulation and speciation in rice with different radial oxygen loss? *Journal Hazardous Material*. http://dx.doi.org/10.1016/j.jhazmat.2012.05.044.

Magyarosy A, Laidlaw R, Kilaas R, Echer C, Clark D, Keasling J, 2002. Nickel accumulation and nickel oxalate precipitation by *Aspergillus niger*. *Applied Microbiology and Biotechnology* **59**: 382–388.

Maldonado-Mendoza IE, Dewbre GR, Harrison MJ, 2001. A phosphate transporter gene from the extra radical mycelium of an arbuscular mycorrhizal fungus *Glomus intraradices* is regulated in response to phosphate in the environment. *Molecular Plante-Microbe Interactions* **14**: 1140–1148.

McGonigle TP, Miller MH, Evans DG, Fairchild GL, Swan JA, 1990. A new method which gives an objective measure of colonization of roots by vesicular-arbuscular mycorrhizal fungi. *New Phytologist* **115**: 495–501.

Meharg AA, Hartley-Whitaker J, 2002. Arsenic uptake and metabolism in arsenic resistant and nonresistant plant species. *New Phytologist* **154**: 29–43.

Meharg AA, 2003. The mechanistic basis of interactions between mycorrhizal associations and toxic metal cations. *Mycological Research* **107**: 1253–1265.

Meng XG, Korfiatis GP, Bang S, Bang KW, 2002. Combined effects of anions on arsenic removal by iron hydroxides. *Toxicology Letters* **133**: 103–111.

Mitsunobu S, Sakai Y, Takahashi Y, 2008. Characterization of Fe(III) (hydr)oxides in arsenic contaminated soil under various redox conditions by XAFS and Mössbauer spectroscopies. *Applied Geochemistry* **23**: 3236–3243.

Miyata N, Tani Y, Iwahori K, Soma M, 2004. Enzymatic formation of manganese oxides by an Acremonium-like hyphomycete fungus, strain KR21-2. *FEMS Microbiology Ecology* **47**: 101–109.

Ortega-Larrocea MP, Xoconostle-Cázares B, Maldonado-Mendoza IE, Carrillo-González R, Hernández-Hernández J, Díaz Garduño M, López-Meyer M, Gómez-Flores L, González-Chávez MC, 2010. Plant and fungal biodiversity from metal mine wastes under remediation at Zimapan, Hidalgo, Mexico. *Environmental Pollution* **158**: 1922–1931.

Ravel B, Newville M, 2005. ATHENA, ARTEMIS, HEPHAESTUS: interactive graphical data analysis for X-ray absorption spectroscopy using IFEFFIT. *Journal of Synchrotron Radiation* **12**: 537–541.

Salt DE, Norton GJ, 2008. Arsenic-eaters: by accident or by design. *New Phytologist* **180**: 8–11.

Schaffer GF, Peterson RL, 1993. Modifications to clearing methods used in combination with vital staining of roots colonized with vesicular-arbuscular mycorrhizal fungi. *Mycorrhiza* **4**: 29–35.

Sharples JM, Meharg AA, Chambers SM, Cairney JWG, 2000. Mechanism of arsenate resistance in the ericoid mycorrhizal fungus *Hymenoscyphus ericae*. *Plant Physiology* **124**: 1327–1334.

Shin H, Shin H-S, Dewbre GR, Harrison MJ, 2004. Phosphate transport in *Arabidopsis*: Pht1;1 and Pht1;4 play a major role in

phosphate acquisition from both low- and high-phosphate environments. *The Plant Journal* **39**: 629–642.
Smedley PL, Kinniburgh DG, 2002. A review of the source, behaviour and distribution of arsenic in natural waters. *Applied Geochemistry* **17**: 517–568.
Smith PG, Koch I, Gordon RA, Mandoli DF, Chapman BD, Reimer KJ, 2005. X-ray absorption near-edge structure analysis of arsenic species for application to biological environmental samples. *Environmental Science & Technology* **39**: 248–254.
Smith SE, Read DJ, 2008. *Mycorrhizal Symbiosis*, 3rd edn. Academic Press, Cambridge, UK.
Smith SE, Christophersen HM, Pope S, Smith FA, 2010. Arsenic uptake and toxicity in plants: integrating mycorrhizal influences. *Plant and Soil* **327**: 1–21.
Srivastava PK, Vaish A, Dwivedi S, Chakrabarty D, Singh N, Tripathi RD, 2011. Biological removal of arsenic pollution by soil fungi. *Science of the Total Environment* **409**: 2430–2442.
St-Arnaud MC, Hamel C, Vimard B, Caron M, Fortin JA, 1996. Enhanced hyphal growth and spore production of the arbuscular mycorrhizal fungus *Glomus intraradices* in an *in vitro* system in the absence of host roots. *Mycological Research* **100**: 328–332.
Su S, Zeng X, Bai L, Li L, Duan R, 2011. Arsenic biotransformation by arsenic-resistant fungi *Trichoderma asperellum* SM-12F1, *Penicillium janthinellum* SM-12F4, and *Fusarium oxysporum* CZ-8F1. *Science of the Total Environment* **409**: 5057–5062.
Ullrich-Eberius CI, Sanz A, Novacky AJ, 1989. Evaluation of arsenate- and vanadate-associated changes of electrical membrane potential and phosphate transport in *Lemna gibba* G1. *Journal of Experimental Botany* **40**: 119–128.
Ultra Jr VUU, Tanaka S, Sakurai K, Iwasaki K, 2007. Arbuscular mycorrhizal fungus (*Glomus aggregatum*) influences biotransformation of arsenic in the rhizosphere of sunflower (*Helianthus annuus* Linn.). *Soil Science & Plant Nutrition* **53**: 499–508.
Webb SM, 2005. Sixpack: a graphical user interface for XAS analysis using IFEFFIT. *Physica Scripta* **T115**: 1011–1014.
Wright SF, Upadhyaya A, 1996. Extraction of an abundant and unusual protein from soil and comparison with hyphal protein of arbuscular mycorrhizal fungi. *Soil Science* **161**: 575–586.
Xia YS, Chen BD, Christie P, Smith FA, Wang YS, Li XL, 2007. Arsenic uptake by arbuscular mycorrhizal maize (*Zea mays* L.) grown in an arsenic-contaminated soil with added phosphorus. *Journal of Environment Sciences* **19**: 1245–1251.